Mutations in the beta-tubulin gene TUBB2B result in asymmetrical polymicrogyria.

Xavier Hubert Jaglin, Karine Poirier, Yoann Saillour, Emmanuelle Buhler,
Guoling Tian, Nadia Bahi-Buisson, Catherine Fallet-Bianco, Françoise
Phan-Dinh-Tuy, Xiang Peng Kong, Pascale Bomont, et al.

Mutations in the beta-tubulin gene TUBB2B result in asymmetrical polymicrogyria

Xavier Hubert Jaglin [1] [†] , Karine Poirier [1] [†] , Yoann Saillour [1] , Emmanuelle Buhler [2] , Guoling Tian [3] , Nadia Bahi-Buisson [1] [4] , Catherine Fallet-Bianco [5] , Françoise Phan-Dinh-Tuy [1] [#] , Xiang Peng Kong [3] , Pascale Bomont [2] , Laëtitia Castelnau-Ptakhine [1] , Sylvie Odent [6] , Philippe Loget [7] , Manoelle Kossorotoff [4] , Irina Snoeck [8] , Ghislaine Plessis [9] , Philippe Parent [10] , Cherif Beldjord [11] , Carlos Cardoso [2] , Alfonso Represa [2] , Jonathan Flint [12] , David Anthony Keays [13] , Nicholas Justin Cowan [3] * , Jamel Chelly [1] *

[1] *IC, Institut Cochin CNRS : UMR8104 , INSERM : U567 , Université Paris Descartes - Paris V , Direction,services Communs,plateformes Bâtiment MECHAIN 22 rue Méchain 75014 PARIS,FR*

[2] *INMED, Institut de neurobiologie de la Méditérranée INSERM : U901 , Université de la Méditerranée , Parc scientifique de Luminy, BP 13, 13273, Marseille Cedex 09,FR*

[3] *Department of Biochemistry New York University Medical Center , New York, NY,US*

[4] *Service de neurologie pédiatrique AP-HP , Université Paris Descartes - Paris V , Hôpital Necker - Enfants Malades , FR*

[5] *Service d'Anatomie Pathologique Hôpital Sainte Anne , Paris,FR*

[6] *Service de génétique médicale CHU Rennes , Hôpital Sud, Rennes,FR*

[7] *Service d'anatomopathologie CHU Rennes , Université de Rennes I , 35000 Rennes,FR*

[8] *Locatie Juliana Kinderziekenhuis Polikliniek Locatie Juliana Kinderziekenhuis Polikliniek , Den Haag,NL*

[9] *Service de génétique CHU Caen , Hôpital Clémenceau , Avenue Georges Clémenceau, Caen,FR*

[10] *Unité d'hémato-oncologie Hôpital des Enfants , Brest,FR*

[11] *Laboratoire de biochimie et génétique moléculaire Hôpital Cochin , AP-HP , Université Paris Descartes - Paris V , FR*

[12] *Wellcome Trust Centre for Human Genetics University of Oxford , Oxford,GB*

[13] *Institute of Molecular Pathology Institute of Molecular Pathology , Vienna,AT*

* Correspondence should be adressed to: Nicholas Justin Cowan <nicholas.cowan@med.nyu.edu >
* Correspondence should be adressed to: Jamel Chelly <jamel.chelly@inserm.fr >

[†] These authors contributed equally to this work

[#] Present address: UMR-S 839, INSERM, Université Pierre et Marie Curie-Paris 6, Institut du Fer à Moulin, 17, rue du Fer à Moulin, 75005 Paris, France.

Abstract

Polymicrogyria is a relatively common but poorly understood defect of cortical development characterized by numerous small gyri and a thick disorganized cortical plate lacking normal lamination. We show an association between bilateral asymmetrical polymicrogyria and de novo mutations in a β-tubulin gene, TUBB2B , in four patients and a 27 GW (gestational week) fetus. Neuropathological examination of the fetus revealed an absence of cortical lamination associated with the presence of ectopic neuronal cells in the white matter, and in the leptomeningeal spaces due to breaches in the pial basement membrane. In utero RNAi-based inactivation demonstrates that TUBB2B is required for neuronal migration. We also show that two disease-associated mutations lead to an impaired formation of tubulin heterodimers. These observations, together with previous data, demonstrate that disruption of microtubule-based processes underlies a large spectrum of neuronal migration disorders that includes not only lissencephaly/pachygyria, but also polymicrogyria malformations.

The crucial role of the tubulin superfamily in diverse cellular processes[1] and the association of TUBA1A mutations with a broad lissencephaly spectrum[2 -4] led us to hypothesize that mutations in other tubulin genes that are highly expressed during CNS development might also result in malformations of cortical development. In a previous screen of agyria/pachygyria patients, we excluded the implication of TUBA1B , TUBA1C and TUBB3 [3]. In this study we report the screening of 3 additional candidate tubulin genes (TUBB2A,B,C) in patients with a wide range of cortical dysgeneses, including polymicrogyria (PMG) syndromes associated with epilepsy and/or neurodevelopmental delay (see Material and Methods section). Although no non-synonymous variations were found either in TUBB2A or in TUBB2C (see alignment in Supplementary Fig. 1), heterozygous missense mutations were found in TUBB2B (Fig. 1a) in four unrelated individuals and one fetus. All mutations, c.514T>C (p.S172P), c.629T>C (p.I210T), c.683T>C (p.L228P), c.793T>C (p.F265L) and c.935C>T (p.T312M) affect residues that are rigidly conserved from yeast to human Supplementary Fig. 2 and reside in exon 4 (Fig. 1a , Table 1). Consistent with a de novo origin of the TUBB2B mutations, none were found in the parents of affected individuals or in 360 normal controls (see referenced polymorphisms in Supplementary Fig. 1). Brain MRI sequences revealed that all patients share the presence of a complex brain dysgenesis with bilateral, asymmetrical, and anteriorly predominant polymicrogyria (PMG), fusion of the caudate and putamen with internal capsule hypoplasia, corpus callosum agenesis or dysgenesis and, in most cases, cerebellar

and pons atrophy (Fig. 1b-j , Table 1 , Supplementary Fig. 3). In addition, neurohistopathological analysis of the fetal brain showed asymmetrical bilateral PMG with the absence of a corpus callosum, several nodular cluster of ectopic neurons in both hemispheres and a disorganization of cortical layering (Fig. 1k-r) including the presence of radial columnar heterotopic neurons in the white matter in the two hemispheres (Fig. 1m). These abnormalities strongly suggest migration defects and perturbations of axon tract formation associated with mutations in TUBB2B . In addition to the typical unlayered polymicrogyric cortex, the analysis of the left hemisphere reveals overmigration of MAP2+ neurons through breaches in the pial basement membrane (BM) (Fig. 1l,n,r and Supplementary Fig. 4). Analysis of radial glial fibers revealed a striking disorganization beyond the pial BM (Fig. 1p). These observations recall the phenotype of mice inactivated for Gpr56 [5], a gene associated with bilateral frontoparietal PMG in humans[6]. The macroscopic aspect and folding of the cerebellum appeared similar to the cerebellum of a control fetus of 27 GW. At the microscopic level, many nodular heterotopia were observed in both cerebellar hemispheres.

To investigate the association between TUBB2B mutations and neuronal migration disorders, we studied the expression of Tubb2b during mouse brain development by in situ hybridization and qRT-PCR and analyzed the consequences on the cortical neuronal migration of TUBB2B loss of function induced by in utero RNA interference.

Sections of embryos at embryonic day 14.5 (E14.5) and 16.5 (E16.5) showed strong labeling restricted to central and peripheral nervous systems (See Supplementary Fig. 5). Using sagittal sections of the brain at E16.5, we found that expression predominated in the cortical plate and also within a thin layer in the subplate, whereas no signal was observed in the marginal zone and fainter labeling was seen in the ventricular and intermediate zones (Supplementary Supplementary Fig. 5a-e). The strong labelling in the developing cortex subsequently decreases after birth although Tubb2b labeling remains intense in the adult cerebellum, hippocampus and olfactory bulb (Supplementary Fig. 5). Taken together these data suggest that Tubb2b is strongly expressed in postmitotic neurons with dominant expression during neuronal migration and differentiation[7 -9], and to a lesser extent in progenitor cells. RT-PCR analysis also showed that Tubb2b is expressed in astro-glial cells and C6 glial cells (data not shown).

We used rat in utero RNAi approach[10] to knock-down Tubb2b expression by about 50 % at embryonic day 15.5 (E15.5), a time coincident with the migration of neurons within the cortex, to mimic the consequence of heterozygous loss of function mutations. We tested different small hairpin RNAs (shRNA) and used two shRNAs targeting either the coding sequence (CDS-sh) or the 3′ untranslated region (3′UTR-sh) that repressed Tubb2b expression in vitro by approximately 60%, while scrambled controls did not destabilize the Tubb2b mRNA (Supplementary Fig. 6a-b). These shRNAs combined with a Red Fluorescent Protein (RFP)-encoding reporter construct were electroporated into progenitor cells located of the ventricular zone (VZ) of E15 rat neocortices. These cells give rise to further young neurons expressing the fluorescent protein as they migrate towards the cortical plate. In E20 brain sections, we observed that neurons electroporated 5 days previously with RFP alone reached the cortical plate as expected (Fig. 2a-b). However in utero expression of 3′ UTR-sh induced a significant arrest of cells within the sub-ventricular zone (SVZ)/intermediate zone (IZ) (Fig. 2c-d,j-k ; stratum 4: $F_{(3,42)}=21.716$, $p<0.0001$; stratum 5:$F_{(3,42)}=20.394$, $p<0.0001$). To further validate the specificity of our results, we performed in utero RNAi with the coding sequence CDS-sh and found that it leads to the same migration arrest (Fig. 2e , Supplementary Fig. 7). We also showed that the expression of both scrambled-sh controls did not disrupt migration (Fig. 2f,g). Finally, we performed a rescue experiment in which we cotransfected a bicistronic construct driving the expression of Tubb2b and Green Fluorescent Protein (GFP) as a reporter. Although the expression of this construct alone does not alter migration (Fig. 2h), it significantly suppresses the blocking effect of 3'UTR-sh on migration (Fig. 2i,k ; strata 8-10: $F_{(3,42)}>23.4$,$p<0.0001$). This RNAi-based approach reinforces the evidence that microtubules act as a critical node during corticogenesis and strongly implicates Tubb2b/TUBB2B in neuronal migration.

To define the functional consequences of the mutations in TUBB2B , we examined the potential implications of each of the mutated residues on the known structure of the β-tubulin polypeptide[11 ,12] (Fig. 3a). S172 resides in a loop that forms part of the guanosine nucleotide-binding site, which when mutated to a proline (S172P) is predicted to disrupt a hydrogen bond and to destabilize the GTP pocket. L228 and F265 are either in the vicinity of or part of the GTP/GDP binding site, with potential consequences for GTP binding. The remaining mutations appear to be less consequential in terms of the GTP binding and overall stability of the protein. Because they are located on the surface, they may interfere with specific partner interactions.

We then investigated the ability of the β-tubulin mutants to produce functional α/β tubulin heterodimers through the complex chaperone-dependent folding pathway[13 ,14] (Fig. 3b) by transcription/translation in rabbit reticulocyte lysate15 . All mutant proteins were translated as efficiently as a wild type control (Fig. 3c). In contrast, analysis under native conditions revealed a range of reaction products (Fig. 3d,e) that could be assigned on the basis of their electrophoretic mobilities[14 ,16]. In the case of TUBB2B mutant proteins, these products frequently differed both quantitatively and qualitatively from the wild type control (See Supplementary Table 1). Most conspicuously, two mutant proteins (p.F265L and p.S172P) completely failed to yield the intermediate corresponding to Tubulinspecific Chaperone A (TBCA)/β-tubulin (Fig. 3d,e). In addition, the yield of native α/β heterodimers produced following a chase with added native tubulin was either slightly reduced (in the case of p.I210T and p.T312M), dramatically reduced (in the case of p.L228P and p.F265L), or undetectable (in the case of p.S172P) (Fig. 3e). (For kinetic analyses, see also Supplementary Results and Supplementary Fig. 8).

We then investigated the ability of the β-tubulin mutants to produce functional α/β tubulin heterodimers through the complex chaperone-dependent folding pathway[13 ,14] (Fig. 3b) by transcription/translation in rabbit reticulocyte lysate15 . All mutant proteins were translated as efficiently as a wild type control (Fig. 3c). In contrast, analysis under native conditions revealed a range of reaction products (Fig. 3d,e) that could be assigned on the basis of their electrophoretic mobilities[14 ,16]. In the case of TUBB2B mutant proteins, these products frequently differed both quantitatively and qualitatively from the wild type control (See Supplementary Table 1). Most conspicuously, two mutant proteins (p.F265L and p.S172P) completely failed to yield the intermediate corresponding to Tubulinspecific Chaperone A (TBCA)/β-tubulin (Fig. 3d,e). In addition, the yield of native α/β heterodimers produced following a chase with added native tubulin was either slightly reduced (in the case of p.I210T and p.T312M), dramatically reduced (in the case of p.L228P and p.F265L), or undetectable (in the case of p.S172P) (Fig. 3e). (For kinetic analyses, see also Supplementary Results and Supplementary Fig. 8].

To examine the mechanism of defective heterodimer assembly of the p.F265L and p.S172P mutant polypeptides in detail, we did reconstituted folding reactions in vitro using purified components[14 ,16]. We observed the generation of TBCD/β-tubulin co-complexes in reactions performed with p.F265L and p.S172P (Fig. 4a) that might be ascribable to the relatively high concentrations of CCT and TBCD in these reactions compared to the more physiological concentrations in reticulocyte lysate. Indeed, when the abundance of TBCD was reduced by a factor of 5 in reactions performed with a constant level of CCT, the yield of the wild type β-tubulin/TBCD co-complex diminished to 25% of the original level, and the F265L β-tubulin/TBCD co-complex was reduced to an undetectable level (Fig. 4c,d). Similar data were obtained for the p.S172P mutation [Supplementary Fig. 9]. We conclude that in addition to a dramatic failure of p.F265L and p.S172P CCT-generated folding intermediates to stably interact with TBCA, these mutations also result in a reduced efficiency of intermediate interaction with TBCD (See also Supplementary Results]. To assess the competence of mutant heterodimers expressed by transcription/translation to incorporate into microtubules, we analyzed their ability to co-cycle with native brain microtubules in vitro and to co-assemble with microtubules upon transfection into cultured cells. In the cases of p.F265L and p.S172P we observed 1) a very low yield of labeled heterodimers incorporated into microtubules and 2) a further diminution between the first (1) and second (2) cycles of polymerization/depolymerization, suggesting significant instability (Fig. 5a). Upon heterologous overexpression by transfection in cultured cells, we found that 3 mutants (p.I210T, p.L228P, p.T312M) behaved indistinguishably from the wild-type protein in that they were efficiently incorporated into interphase microtubules (data not shown). In contrast, in the case of the p.S172P and p.F265L mutants, there was scant evidence of incorporation into well-defined microtubules (Fig. 5b) (See also Supplementary Results for assessment of microtubule dynamics). Taken together, these experiments show that p.S172P and p.F265L are significantly compromised in their ability to properly assemble into microtubules in vivo , and are consistent with our in vitro transcription/translation experiments in which neither of these mutant proteins yielded significant amounts of polymerization competent heterodimers (Fig. 3e , 5a).

We further sought to test whether expression of the p.S172P and unrelated p.T312M mutants in vivo could complement the phenotype caused by knockdown of Tubb2b . We electroporated the pCAGIG-p.S172P(or p.T312M)-Tubb2b -IRES-GFP construct either alone or in combination with the 3′UTR-sh and analyzed the position of electroporated cells within the cortex. We found that, although expression of each mutant alone does not massively affect migration (Fig. 5e,g), expression of each mutant in the knock-down context maintains the cells stalled within the SVZ/IZ (Fig. 5f,h) and fails to complement the RNAi effect.

In this study, we implicate mutations in TUBB2B as causative of brain malformations encompassing asymmetrical PMG associated with an unlayered cortex, heterotopic neuronal cells in the white matter and neuronal overmigration through the pial BM. It is worthwhile mentioning that corpus callosum dysgenesis, dysmorphic basal ganglia, cerebellum dysplasia and brainstem hypoplasia are common features to TUBA1A -related agyria/pachygyria and TUBB2B -related PMG. Mutations in GPR56 and SRPX2 genes are also known to be associated with PMG. However the diagnosis of TUBB2B -related PMG could be evoked through assessment of clinical and imaging criteria highlighted in Supplementary Table 2 .

Our in vitro data show that the five newly discovered disease-associated TUBB2B mutations involve a spectrum of tubulin heterodimer assembly defects (summarized in Supplementary Table 1) leading to loss of function in the cases of p.S172P and p.F265L. The two most severe defects observed in vitro (p.S172P and p.F265L) are associated with the most and the least severe clinical phenotypes, respectively, suggesting that there is no simple correlation in the panel of 5 mutated patients. We also establish that loss of function is associated in vivo with defective migration and mislocalization of developing neurons within the cortex, suggesting that TUBB2B -related forms of PMG are primarily due to haploinsufficiency, though dominant negative effect can not be excluded for the

p.S172P mutation. For those mutations that have less or no apparent impact on tubulin heterodimer assembly, the functional defect seems likely to concern a subtle effect on either microtubule dynamics, or on the interaction with one or more microtubule interacting proteins (MAPs) that are critical for proper cortical neuronal migration, or both. The cellular consequences of TUBB2B mutations, and the mechanisms by which this results in polymicrogyria, an unlayered cortex, and heterotopic neuronal cells remain unknown. We propose that the neuropathophysiology of TUBB2B -related PMG might result from a combination of both neuronal migration impairment and radial glia dysfunction that lead respectively to ectopic neurons in the white matter and cerebellum, and to pial membrane breaches (see Supplementary Discussion).

In higher eukaryotes, α- and β-tubulins are encoded by a multigene family that are evolutionary conserved[17] among different species and are differentially expressed[18 ,19]. To explain the need for these highly conserved multiple genes, it has been hypothesized that the different isotypes may be required to form specific sets of microtubules that carry out unique functions18. Though this hypothesis is still a matter of debate, our data showing that mutations in TUBA1A and TUBB2B are associated with different gyral abnormalities argue in favor of specific roles of TUBB2B and TUBA1A during corticogenesis and neuronal migration (see Supplementary Table 2). It is also possible that subtle differences of spatio-temporal profiles of TUBA1A and TUBB2B expression (i.e. populations of interneurons, radial glia cells and astro-glial cells) may account for some of the cortical phenotypic differences.

METHODS

Patients and Analysis of TUBB2B

Patients' DNA or blood samples and informed consent (from all patients' parents) were obtained according to the guidelines of local institutional review boards at Cochin Hospital and INSERM (French National Institute of Health and Medical Research). TUBB2B was screened in a total of 168 sporadic cases selected with clinical and brain imaging features compatible with a diagnosis of either lissencephaly (n=120) or polymicrogyria syndromes (n=48). Patients with lissencephaly included those with agyria/pachygyria (n=105) or subcortical laminar heterotopia (n=15) with (n=13) or without (n=107) cerebellar hypoplasia or dysplasia. In addition to this cohort of living patients, we also screened TUBB2B in 5 fetuses (using DNA samples derived from skin tissue), which had been sent to our diagnostic center after medical abortions and neuropathological analyses (See details in Supplementary Methods section).

Neuropathological procedures

Neuropathological analyses were performed on 5 fetuses (aged from 23 to 35 gestational weeks) in accordance with French law. Briefly, after removal from the skull, each brain was fixed in 10% (v/v) formaldehyde solution containing NaCl (9 g/l) and $ZnSO_4$ (3 g/l) for a variable time (depending on the volume of the brain) from 3 to 6 weeks. Brains were cut in a coronal plane and sections involving one or both hemispheres were embedded in paraffin. Paraffin blocks were sectioned into either 5 μm (brainstem and cerebellum) or 8–10 μm (hemispheres) thick sections and stained using standard methods for histological and immunohistological studies.

RNAi constructs

We performed RNAi experiments using 2 different oligonucleotides targeting the coding sequence or the 3′UTR of rat Tubb2b : CDS-sh (#318-341) and 3′UTR-sh (#1553-1576). A BLAST search against databases confirmed the specificity of each target. Annealed oligonucleotides were cloned into a mU6-pro vector[20]. For the rescue experiment, we subcloned the coding sequence of Rattus norvegicus Tubb2b cDNA (IMAGE 5599369) without the UTRs, into the pCAGIG vector[21] (Addgene plasmid 11159, Cambridge, MA), such that a CMV immediate early enhancer/chicken β-actin promoter (CAG) drives transcription of the bicistronic Tubb2b -IRES-GFP mRNA. The rescue experiment allows the expression of a 3′UTR targeting shRNA in combination with the overexpression construct. It implies that the overexpressed Tubb2b RNA is resistant to the ShRNA as the target (3′UTR) is absent.

In utero electroporation

Wistar rats (Janvier, Le Genest Saint Isle, France) were mated, maintained and used in our animal facilities in agreement with European Union and French legislation. Timed pregnant rats [embryonic day 15 (E15)–E16; E0 was defined as the day of confirmation of sperm-positive vaginal plug] were anesthetized with ketamine/xylazine (respectively 0.1 and 0.01 mg per g body weight). The uterine horns were exposed, and a lateral ventricle of each embryo injected via pulled glass capillaries and a microinjector (Picospritzer II; General Valve Corp., Fairfield, NJ) with Fast Green (2 mg/ml; Sigma, St. Louis, MO) combined with the following DNA constructs: 0.5 μg/μl pCAGGS-red fluorescent protein (mRFP) either alone or with 1.0 μg/μl of shRNA construct targeting the Tubb2b mRNA. Plasmids were further electroporated by discharging a 4000 μF capacitor charged to 50 V with a BTX ECM 830 electroporator (BTX Harvard Apparatus, Holliston, MA). The voltage was discharged in 5 electric pulses at 950 ms intervals via 5 mm electrodes placed on the head of the embryo across the uterine wall. We performed in utero electroporation in embryonic rats at E15.5. This moment corresponds to an active period of both radial and tangential migration of newborn neurons in the cortex.

Protein modeling

A model of human β-tubulin was built by homology modeling using available structures (Research Collaboratory for Structural Bioinformatics PDB code 1TUB) from Nogales et al.[11 ,12]. The image in Figure 3a was rendered using PyMOL (http://www.pymol.org).

In Vitro translation

Transcription/translation reactions were performed at 30°C for 60 min in 25 μl of rabbit reticulocyte lysate (TnT T7 Quick Coupled Transcription/Translation System, Promega, Madison, WI) containing 35S-methionine (specific activity 1,000 Ci/μmol; 10 μCi/l) using TUBB2B wild-type and mutant cloned into the pET-23b(+) vector (Novagen, Madison, WI) as templates. For the generation of labeled heterodimers, transcription/translation reactions were chased for a further 2 h at 30°C by the addition of native bovine brain tubulin at 0.2 mg/ml. Labeled reaction products were detected by autoradiography after resolution on either SDS-PAGE or on native polyacrylamide gels as described[14 ,16].

In Vitro Folding Reactions

In vitro folding assays were performed either directly in the rabbit reticulocyte translation cocktail, or in folding buffer containing CCT (cytosolic chaperonine), ATP, GTP and tubulin chaperones (TBCB, TBCC, TBCD, TBCE) as described previously[16]. Target proteins (i.e. wild type or mutant forms of TUBB2B β-tubulin) were expressed as 35S-labeled proteins in BL21 DE3 pLysS cells[22] (Invitrogen, Carlsbad, CA) and the inclusion bodies purified and unfolded in denaturant following previously described procedures[23]. Reaction products were further analyzed by electrophoresis on native polyacrylamide gels[14 ,16]. In some experiments, the yield of various reaction products was determined using a phosphorimager (Personal Molecular Imager, Bio-Rad Laboratories, Hercules, CA).

Microtubule Co-polymerization Experiments

Products of in vitro translation reactions were mixed with depolymerized bovine brain microtubules and taken through successive cycles of polymerization and depolymerization as described[24]. At the end of each cycle, aliquots containing equal amounts of depolymerized material were removed and analyzed by SDSPAGE and autoradiography.

Cell Culture, Transfections and Immunofluorescence

Constructs were transfected into COS-7 cells grown on glass coverslips in Dulbecco's Modified Eagle's Medium containing 10% (v/v) fetal calf serum using the FuGENE6 transfection reagent (Roche Applied Science, Indianapolis, IN). Twenty-four hours post-transfection cells were fixed with −20°C methanol. Immunostaining was performed with a polyclonal anti-FLAG antibody (to visualize protein expressed from the construct; Sigma-Aldrich Inc., St. Louis, MO) and a monoclonal anti-α-tubulin antibody (to visualize the overall microtubule network; DM1A, Sigma-Aldrich Inc., St. Louis, MO).

Footnotes:

Author contributions: J.C. coordinated and instigated the study with D.A.K. and J.F.. X.H.J. performed biochemical, cellular and in vivo functional studies. N.B.B., K.P. and C.F.B recruited cases and controls. N.B.B., C.F.B., S.O., P.L., M.K., I.S., G.P., P.P. and C.B. helped in collecting the patients. K.P., D.A.K. and Y.S. screened the subject DNAs and performed the genetic analyses. C.F.B. performed the neuropathological analyses. G.T. and N.J.C. provided reagents and expertise for the biochemical study; X.P.K. helped us to compute and analyze the structural issues; C.C., E.B., P.B. and A.R. provided expertise and technical assistance for in utero RNAi analysis. F.P.D.T. and K.P. performed the RNA ISH analysis. X.H.J. and K.P. drafted the manuscript with the help of N.J.C. and J.C.

References:

- 1 . Dutcher SK . The tubulin fraternity: alpha to eta . Curr Opin Cell Biol . 13 : 49 - 54 2001 ;
- 2 . Keays D.A . Mutations in alpha-tubulin cause abnormal neuronal migration in mice and lissencephaly in humans. . Cell . 128 : 45 - 57 2007 ;
- 3 . Poirier K . Large spectrum of lissencephaly and pachygyria phenotypes resulting from de novo missense mutations in tubulin alpha 1A(TUBA1A). . Hum Mutat . 28 : 1055 - 64 2007 ;
- 4 . Bahi-Buisson N . Refinement of cortical dysgeneses spectrum associated with TUBA1A mutations . J Med Genet . 45 : 647 - 53 2008 ;
- 5 . Li S . GPR56 regulates pial basement membrane integrity and cortical lamination . J Neurosci . 28 : 5817 - 26 2008 ;
- 6 . Piao X . G protein-coupled receptor-dependent development of human frontal cortex . Science . 303 : 2033 - 6 2004 ;

- 7 . Kriegstein AR , Noctor SC . Patterns of neuronal migration in the embryonic cortex . Trends Neurosci . 27 : 392 - 9 2004 ;
- 8 . Marin O , Rubenstein JL . A long, remarkable journey: tangential migration in the telencephalon . Nat Rev Neurosci . 2 : 780 - 90 2001 ;
- 9 . Metin C , Baudoin JP , Rakic S , Parnavelas JG . Cell and molecular mechanisms involved in the migration of cortical interneurons . Eur J Neurosci . 23 : 894 - 900 2006 ;
- 10 . Bai J . RNAi reveals doublecortin is required for radial migration in rat neocortex . Nat Neurosci . 6 : 1277 - 83 2003 ;
- 11 . Nogales E , Whittaker M , Milligan RA , Downing KH . High-resolution model of the microtubule . Cell . 96 : 79 - 88 1999 ;
- 12 . Nogales E , Wolf SG , Downing KH . Structure of the alpha beta tubulin dimer by electron crystallography . Nature . 391 : 199 - 203 1998 ;
- 13 . Lewis SA , Tian G , Cowan NJ . The alpha- and beta-tubulin folding pathways . Trends Cell Biol . 7 : 479 - 84 1997 ;
- 14 . Tian G . Pathway leading to correctly folded beta-tubulin . Cell . 86 : 287 - 96 1996 ;
- 15 . Cleveland DW , Kirschner MW , Cowan NJ . Isolation of separate mRNAs for alpha- and beta-tubulin and characterization of the corresponding in vitro translation products . Cell . 15 : 1021 - 31 1978 ;
- 16 . Tian G . Tubulin subunits exist in an activated conformational state generated and maintained by protein cofactors . J Cell Biol . 138 : 821 - 32 1997 ;
- 17 . Little M , Seehaus T . Comparative analysis of tubulin sequences. . Comp Biochem Physiol B . 90 : 655 - 70 1988 ;
- 18 . Luduena RF . Are tubulin isotypes functionally significant. . Mol Biol Cell . 4 : 445 - 57 1993 ;
- 19 . Sullivan KF , Cleveland DW . Identification of conserved isotypedefining variable region sequences for four vertebrate beta tubulin polypeptide classes . Proc Natl Acad Sci U S A . 83 : 4327 - 31 1986 ;
- 20 . Yu JY , DeRuiter SL , Turner DL . RNA interference by expression of short-interfering RNAs and hairpin RNAs in mammalian cells . Proc Natl Acad Sci U S A . 99 : 6047 - 52 2002 ;
- 21 . Matsuda T , Cepko CL . Electroporation and RNA interference in the rodent retina in vivo and in vitro . Proc Natl Acad Sci U S A . 101 : 16 - 22 2004 ;
- 22 . Studier FW , Rosenberg AH , Dunn JJ , Dubendorff JW . Use of T7 RNA polymerase to direct expression of cloned genes . Methods Enzymol . 185 : 60 - 89 1990 ;
- 23 . Gao M , Knipe DM . Distal protein sequences can affect the function of a nuclear localization signal . Mol Cell Biol . 12 : 1330 - 9 1992 ;
- 24 . Tian G . A Pachygyria-causing {alpha}-Tubulin Mutation Results in Inefficient Cycling with CCT and a Deficient Interaction with TBCB . Mol Biol Cell . 19 : 1152 - 61 2008 ;
- 25 . Cowan NJ , Lewis SA . Type II chaperonins, prefoldin, and the tubulinspecific chaperones. . Adv Protein Chem . 59 : 73 - 104 2001 ;
- 26 . Vainberg IE . Prefoldin, a chaperone that delivers unfolded proteins to cytosolic chaperonin. . Cell . 93 : 863 - 73 1998 ;
- 27 . Spiess C , Meyer AS , Reissman S , Frydman J . Mechanism of the eukaryotic chaperonin: protein folding in the chamber of secrets. . Cell Biol . 14 : 598 - 604 2004 ;
- 28 . Tian G , Vainberg IE , Tap WD , Lewis SA , Cowan NJ . Quasi-native chaperonin-bound intermediates in facilitated protein folding. . J Biol Chem . 270 : 23910 - 3 1995 ;

Figure 1

Magnetic Resonance Imaging and Histopathology Analysis of Patients with TUBB2B mutations

(a) Linear representation of the β-tubulin protein showing the position of heterozygous PMG-associated mutations. (b–j) Representative brain imaging features of 3 patients carrying TUBB2B mutations: P2 (p.L228P) (b-d); P3 (p.F265L) (e-g); P1 (p.T312M) (h-j). Axial images show areas of PMG that appear more severe in frontal and parietal lobes (b,e) and involve the perisylvian region (e,h). The PMG appears either mildly (b,h) or severely asymmetric with left-sided predominance (e) (Hatched lines highlighted by arrowheads show some of the PMG areas). Basal ganglia appear dysmorphic with a fusion of caudate and putamen, and apparent absence of the anterior arm of the internal capsule (b,e,h). Midline sagittal section shows corpus callosum agenesis (c), hypogenesis and abnormal thickness (f), or dysmorphy with a flat shape (i), associated with mild to severe cerebellar vermis hypoplasia or atrophy (c,f,i) and with brainstem hypoplasia (double asterisks). Axial section at the level of the cerebellum and temporal lobes show severe vermian dysplasia (d,j) or atrophy (g) (black asterisks). (k–n,q,r) Nissl-stained sections of the 27GW fetus (p.S172P mutation) brain display asymmetrical bilateral polymicrogyria (black arrows in k,l) with callosal agenesis. Left and right hemispheres present respectively typical unlayered polymicrogyric cortex (l,n) and focal polymicrogyria with a completely disorganized cortex and radial neuronal heterotopias (black arrows in k,m). Several nodular heterotopic neuron clusters were also observed in both hemispheres. Sections of cortical regions of left hemisphere probed for vimentin (o,p) or stained by Nissl (q,r) respectively show either abnormalities of radial glial fiber organization (p) or a disorganized cortex (r) with neuronal overmigration through the pial basement membrane into the leptomeningeal space (black arrows in r). Sections (o,q) correspond to a 27GW control fetus. M: meninges. Scale bars: (k–n) 500 μm, (o–r) 100 μm.
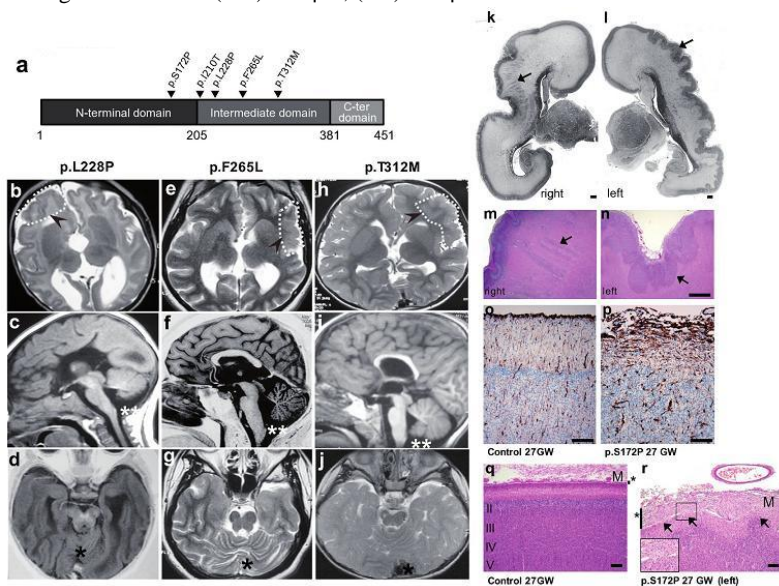
Figure 2

In Utero Knock-Down of rat Tubb2b Expression by RNAi Alters Neuronal Migration in the Isocortex

(a-i) Nissl staining on coronal sections of E20 brains reveals the overall organization of the cortex (a) 5 days after electroporation of a RFP coding reporter construct either alone (b) or in combination with 3′UTR-sh (c, overlay with Nissl in d), CDS-sh (e), or their corresponding scrambled controls (f,g). A rescue experiment was performed using CAG-Tubb2b -IRES-GFP transfected either alone (h, GFP), or combined with 3′UTR-sh (i, GFP). (j,k) Fluorescence intensities reflecting cell positions were converted into gray values and measured across cortices from the VZ to the MZ (j, 3′UTR-sh). k, Bars represent the mean ± SEM of fluorescence intensities in 10 strata dividing the thickness of cortices of independent brains (RFP n=5, 3′UTR-sh n=6, CDS-sh n=6, Scrambled 3′UTR-sh n=4, Scrambled CDS-sh n=5, Rescue n=6). Knockdown of Tubb2b using both hairpins between E15 and E20 disrupts neuronal migration (c,d,e). RFP positive cells are significantly stalled within the deep layers of the cortex (c,k, strata 4,5: $F_{(3,42)} > 20.4$, $p < 0.0001$; $p < 0.001$(***) for 3′UTR-sh compared by Tukey-Kramer test to RFP, scrambled 3′UTR-sh and Rescue respectively) that correspond to the SV/IZ (d, higher magnification) whereas neurons have already reached the CP in control conditions (b,f,g). Tubb2b overexpression preserves neuronal migration (h) showing that migration disruption is a specific consequence of Tubb2b RNAi as it rescued the defect (i,k strata 8-10: $F_{(3,42)} > 23.7$, $p < 0.0001$, $p < 0.001$(***) for 3′UTR-sh compared by Tukey-Kramer test to RFP and Rescue respectively). Hatched lines in (b,c,e-i) correspond to the outer/ventricular limits of the cortex. Scale bars : 200 µm (a-i).
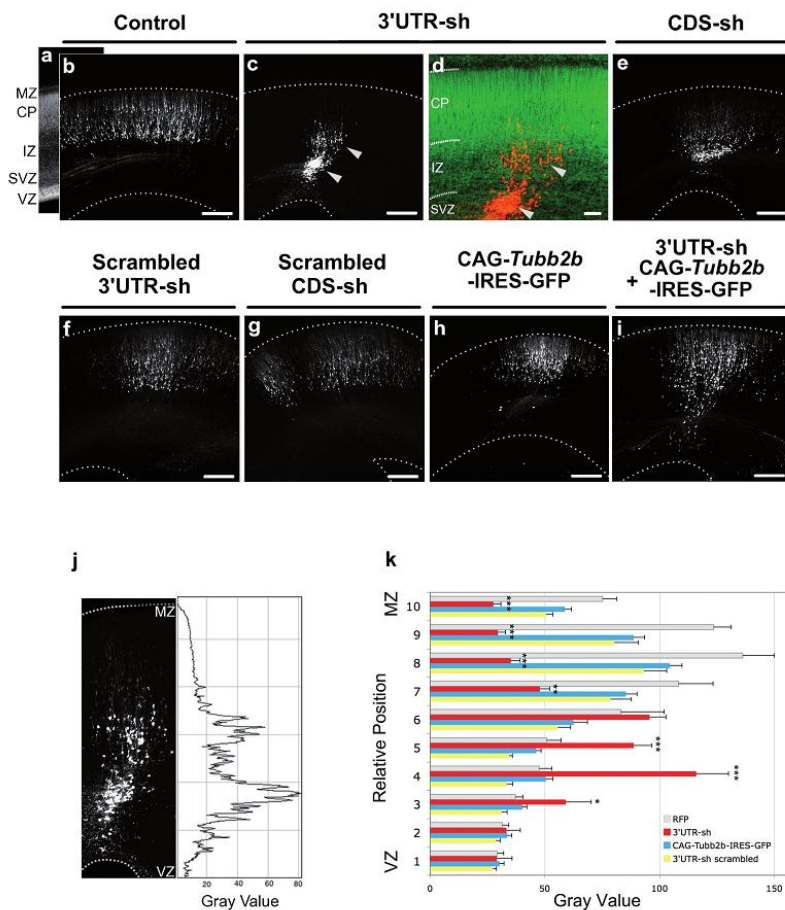
Figure 3

Various Mutations in TUBB2B Result in Inefficient α/β Tubulin Heterodimer Formation In Vitro

(a) Ribbon presentation illustrating placement of side chains of mutated residues (shown in red) and the E-site guanine nucleotide (shown in orange) within the structure of the -tubulin polypeptide[11 ,12].S172 resides between two proline residues in a loop. **(b)** The tubulin folding pathway involves a series of molecular chaperones whose function is to facilitate the assembly of the α/β tubulin heterodimer[25]. Newly translated α-tubulin (α) and β-tubulin (β) polypeptides are first captured and stabilized by prefoldin (PFD) that acts as a shuttling protein to deliver its bound target protein to the cytosolic chaperonin (CCT)[26]. CCT generates productive quasi-native folding intermediates which interact with a set of downstream Tubulin-specific Chaperones (TBCs)[27]. TBCB and TBCE capture CCT-generated α-tubulin intermediates in which the encapsulating GTP-binding pocket (the N-site) is already formed28 producing TBCB/α-tubulin (B/α) and TBCE/α-tubulin (E/α) cocomplexes. TBCA and TBCD capture and stabilize CCT-generated β-tubulin intermediates forming TBCA/β-tubulin (A/β) and TBCD/β-tubulin (D/β) cocomplexes. TBCD/β-tubulin (D/β) and TBCE/α-tubulin (E/α) converge to form a supercomplex with TBCC (C-D/βE/α). Interaction with TBCC (C) results in the triggering of GTP hydrolysis by β-tubulin16. This reaction acts as a switch to signal the release of newly formed GDP-bound α/β heterodimers, which are then competent for incorporation into microtubules. **(c-e)** Analysis by SDS-PAGE (c) or non-denaturing gels (d,e) of in vitro transcription/translation products performed with wild-type (WT) and mutant TUBB2B and further chased with bovine brain tubulin so as to generate α/β tubulin heterodimers (e). The different migration pattern for p.L228P in (c) can be explained by the substitution of a proline in place of leucine, disrupting the helix, and presumably resulting in a change in the binding of SDS and hence a slight change in migration rate on the SDS gel. Note that p.F265L and p.S172P mutants yielded either only a trace or no discernable amount of α/β heterodimer. The remaining mutants all generated products present in the WT control, but in varying yield (d,e).
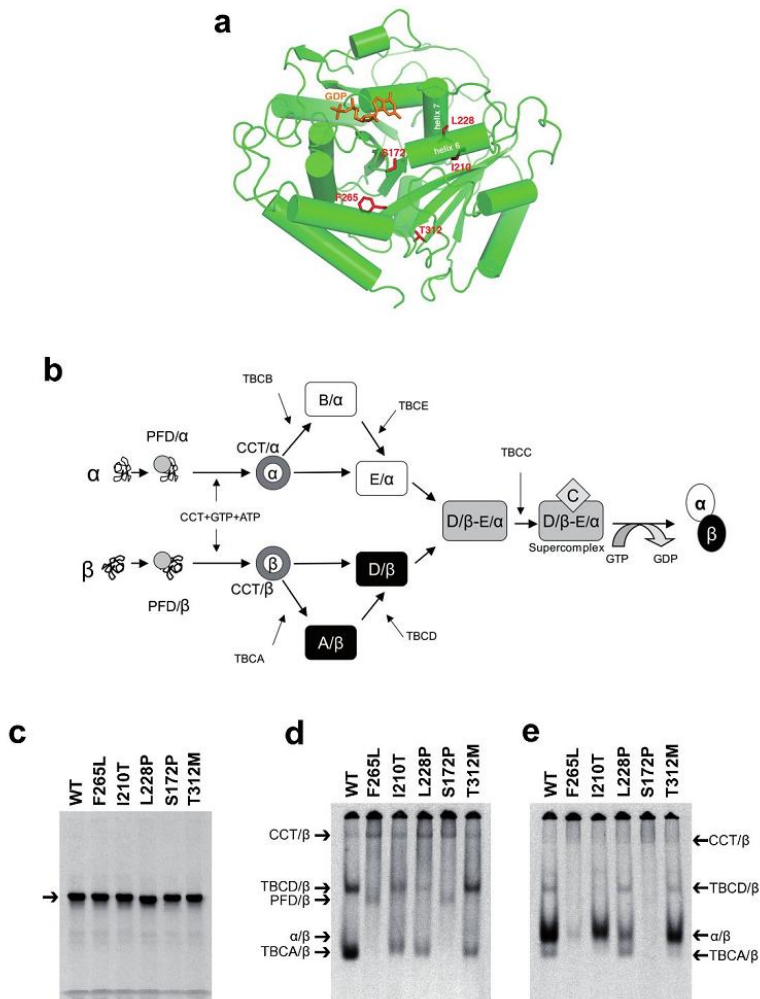
Figure 4

In Vitro Reactions Reveal a Lowered Affinity of p.S172P TUBB2B for TBCD

(a) Analysis on non-denaturing gels of the products of reconstituted folding reactions containing ATP, GTP and various combinations of the purified components that are essential to the heterodimer assembly reaction. **(b–c)** Analysis on non-denaturing gels of the products of in vitro folding reactions performed with ^{35}S-methionine-labeled, unfolded wild type (WT) or p.F265L mutant protein. Reactions contained a range of concentrations of purified cytosolic chaperonin (CCT) (1x, 0.5x, 0.2x) in the presence of constant (1x molar equivalent) TBCD (control reaction) (b) or a range of concentrations of purified TBCD (1x, 0.5x, 0.2x) in the presence of constant (1x molar equivalent) CCT (c). **(d)** Quantitation of the data shown in (b) and (c). Note that when the abundance of TBCD was reduced by a factor of 5 in reconstituted reactions performed with a constant level of CCT, the yield of the TBCD/β-tubulin co-complex declined in the case of the wild type protein to 25% of the original level, but declined to an undetectable level in the case of p.F265L. Similar data were obtained in the case of the p.S172P mutation (Supplementary Fig. 8). The level of radioactivity present in complexes at the 1x concentration is taken as 100. Bars represent the average of two experiments. Arrows in (a–c) denote the migration positions of the CCT/β-tubulin binary complex, the TBCD/β-tubulin co-complex, the native tubulin heterodimer (α/β).
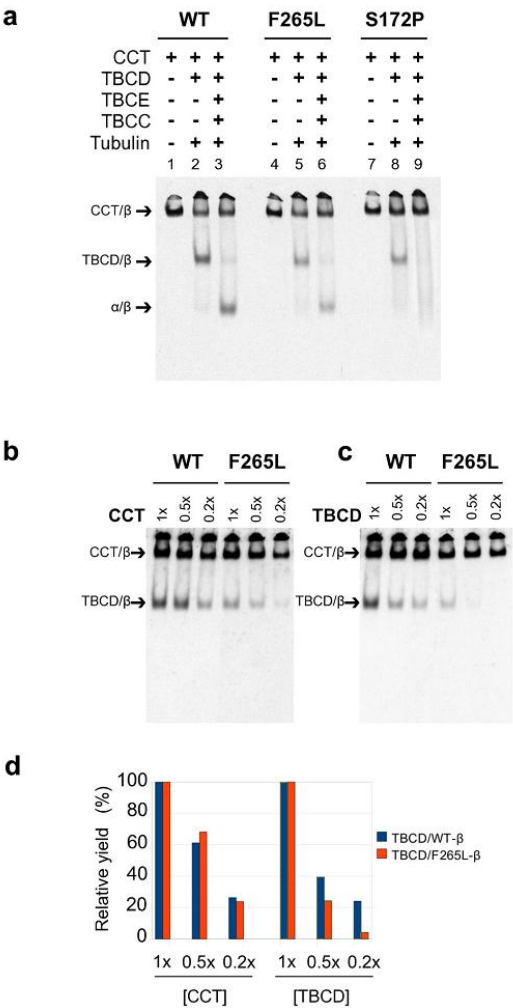
Figure 5

Loss of function of mutant TUBB2B in vitro , in cultured cells and in vivo .

(a) Copolymerization of labeled translation products with native bovine brain microtubules. Aliquots from two successive polymerization/depolymerization cycles (1 and 2), show inefficient incorporation for F265L, L228P and S172P mutants. **(b)** Expression of C-terminally FLAGtagged wild-type and mutant (p.S172P and p.F265L) TUBB2B in vivo after construct transfection into COS-7 cells. Note that F265L and S172P mutants do not incorporate into the MT network. **(c-h)** Nissl staining on coronal sections of E20 brains reveals the overall organization of the cortex (c), and repartition of GFP+ cells within the E20 cortices thickness, on coronal sections (d-h). Expression of p.T312M and p.S172P either alone (e,g) or in combination with 3′UTR-sh (f,h). Note that the over-expression of these mutants in combination with the hairpin does not rescue the neuronal migration defect caused by the RNAi (e,f) although the expression of each mutant alone does not lead to a major migration defect. However, we can see that upon expression of p.S172P a few cells seem to be blocked within the IZ suggesting that p.S172P could have a dominant effect leading to slight migration impairments. Scale bar: 200 μm.
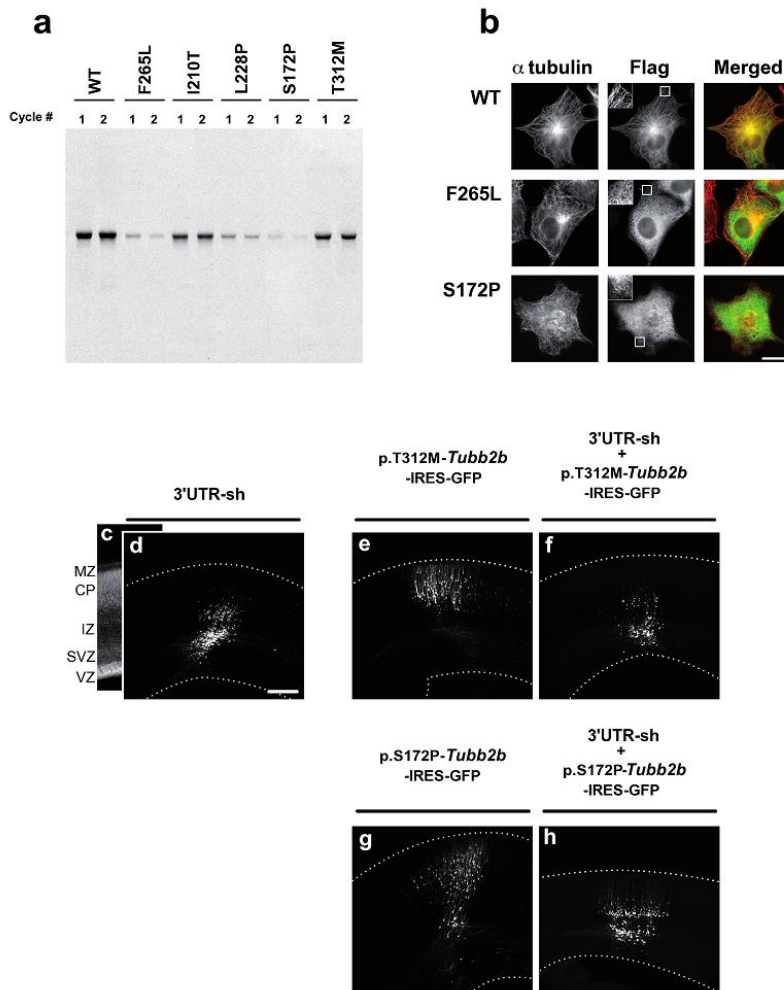
Table 1

Summary of clinical and imaging phenotypes associated with mutations in TUBB2B.

Sex Mutation	P1 Male c.935C>T (P.T312M)	P2 Male c.683T>C (p.L228P)	P3 Male c.793T>C (p.F265L)	P4 Male c.629T>C (p.I210T)	Male Fetus c.514T>C (p.S172P)
Age at last evaluation	2 years	2 years	37 years	13 years	27 weeks of gestation
OFC at birth (or brain weight at medical abortion)	33 cm	31 cm	31 cm	31 cm	Weight approx. 5th percentile
OFC at last examination (percentile)	45 cm (< −3 SD)	43.5 cm (< −3 SD)	51 cm (< −3 SD)	<< −3 SD	NA
Motor/communication skills at last examination	Severe neuromotor impairment (tetraparesis) Walks with aid, unskilful manipulation /Limited language	Severe neuromotor impairment (tetraplegia) Sits with aid, unskilful manipulation /No visual contact	No neuromotor impairment (no diplegia, no tetraplegia) Sentences, severe mental retardation	Severe neuromotor impairment (tetraparesis) Walks with aid, unskilful manipulation /Limited language	NA
Epilepsy	No seizures	Infantile spasms (3 months)	Generalized occasional seizures	Generalized seizures	NA
Gyral pattern	Polymicrogyria	Polymicrogyria	Polymicrogyria	Polymicrogyria	Polymicrogyria
Major location	Predominant in left frontal and parietal lobes	Predominant in frontal and temporal lobes (including the hippocampus)	Asymmetrical, predominant in left frontal, parietal and temporal lobes (including the hippocampus)	Asymetrical, predominant in left frontal, parietal and temporal lobes	Bilateral and asymmetrical, fronto-temporal
Basal ganglia	Dysmorphic caudate and striatum	Dysmorphic caudate and striatum	Dysmorphic caudate and striatum	Dysmorphic caudate and striatum	Normal
Cerebellum	Vermian dysplasia	Vermian dysplasia with hypoplasia	Severe global atrophy	Vermian dysplasia with hypoplasia	Heterotopic neuronal cells
Corpus callosum	Flat shape and hypogenetic	Complete agenesis	Partial posterior agenesis	Atrophy and posterior agenesis	Agenesis
Brainstem	Mild hypoplasia predominant in pons	Mild hypoplasia	Hypoplasia predominant in pons	Hypoplasia predominant in pons	Normal

NA, nonapplicable.